Lessons Learned from Radiation Induced Effects on Solid State Recorders (SSR) and Memories

DRAFT

Christian Poivey, George Gee
SGT-Inc

Janet Barth, Ken LaBel, Harvey Safren
NASA-GSFC

December 2002

Table of Content

1 Background

1.1 Introduction

Solid State Recorders (SSR) have replaced the electromechanical tape recorders to store on board science and engineering data in the early nineties. They provided increased data storage capacity for a reduced power and weight. However SSR uses commercial, non-hardened, memories that are particularly susceptible to the space radiation environment. Because of this, radiation mitigation techniques have been implemented, and these systems have been monitored for radiation effects such as Single Event Upsets (SEU) and Multiple Bit Upset (MBU). Thus, as a by product of the monitoring tasks which form a normal part of a spacecraft's "house-keeping" process, useful data [1-8] has been gathered the last ten years on the radiation tolerance of memories used in the SSRs. In the same way, SEU data has also been gathered on On Board Computer (OBC) memories[9-10].
In addition specific non-hardened memory experiments [11-22] have been flown that give additional information.

1.2 Radiation effects and memories

1.2.1 Single Event Effects

1.2.1.1 Destructive Events

Modern memories are potentially sensitive to Single Event Latchup (SEL) like all CMOS devices. Generally the risk of SEL in space is limited to heavy ions and devices fabricated on epitaxial substrates are less prone to be sensitive to SEL. However some devices fabricated on epitaxial substrates exhibit SEL sensitivity [23-25], and protons could induce latchup in sensitive technologies [26-29].
As gate oxide thickness and feature sizes decrease Single Hard Errors (SHE) have been observed on memories. We can distinguish two types of SHE: first, stuck memory cells due to local total ionizing dose deposition ("microdose") [30-32], second, SEGR failures. SEGR failures have been observed on DRAMs [33] and EEPROM, flash PROMs [34,35,36]. EEPROM are more sensitive during write/programming operation because of the higher voltages applied on thin oxides during these operations [37].

1.2.1.2 Non Destructive Events

SRAMs and DRAMs are extremely sensitive to heavy ion and proton induced Single Event Upset (SEU).
They are also sensitive to Single Event Multiple Bit Upsets (MBU) by the following mechanisms:

- diffusion of charge to closely spaced junctions that upsets several neighboring cells [38,39].
- a particle striking a memory at a grazing angle of incidence, that intersects several sensitive regions and cause multiple upsets [39,40].
- a particle strike in the interface and/or control circuitry of the device that cause large row column errors or block errors [39, 41, 42, 43]. This type of error may lead to Single Event Functional Interrupts (SEFI) that need a reset or even a power cycling to restore nominal operations of the device. Complex state of the art memories like SDRAMs are significantly sensitive to SEFI [44].

EEPROMs and flash EPROM memory cells are not altered by heavy ions and protons in read mode, but Single Event Transient (SET) in the peripheral circuitry induce reading errors on one or several bits of a data word [36,45]. In write or programming mode, these devices are extremely sensitive and this can result in a significant number of programming errors: single bit errors or block errors and even SEFI [35,36].

1.2.2 Total Dose Effects

SRAMs and DRAMs are sensitive to Total Ionizing Dose (TID). The first effect of TID at the device level is a significant increase of the standby current, and a decrease of the retention time of DRAMs, followed by the lost of bits (stuck bits) [46-48]. As for other commercial devices, the TID sensitivity varies significantly for different device types and also for different devices of the same type. The increase of standby current is noticeable after a few krad and the first memory cell in error appears after a total dose level ranging from 8 to >100 krad depending on the device type [46-49].

EEPROMs and flash EPROM are also sensitive to TID. The degradation is higher when exposed to radiation during programming operation. When the parts are irradiated in read mode they can withstand TID levels ranging from 5 to 30 krads without functional failures, but they may fail programming operations after a few krad [36, 50-51].

2 Flight Data

2.1 Introduction

Table 1 lists all the flight data on memories available in the literature. It gives information about the spacecraft name, the type of flight data (data on SSR memory, OBC memory, or experiment), the memory size, the type of memory, the part type and manufacturer, the period of flight and the type of orbit. Fig. 1 plots the periods of flight of the data listed in Table 1. The available data covers more than a full solar cycle on different types or orbits: L2 and GEO orbits exposed to GCR and solar particles, LEO polar orbits exposed to GCR and solar particles and also trapped protons in the South Atlantic Anomaly, and finally LEO inclined orbits, less exposed to GCR and solar particles but more exposed to the trapped particles radiation.

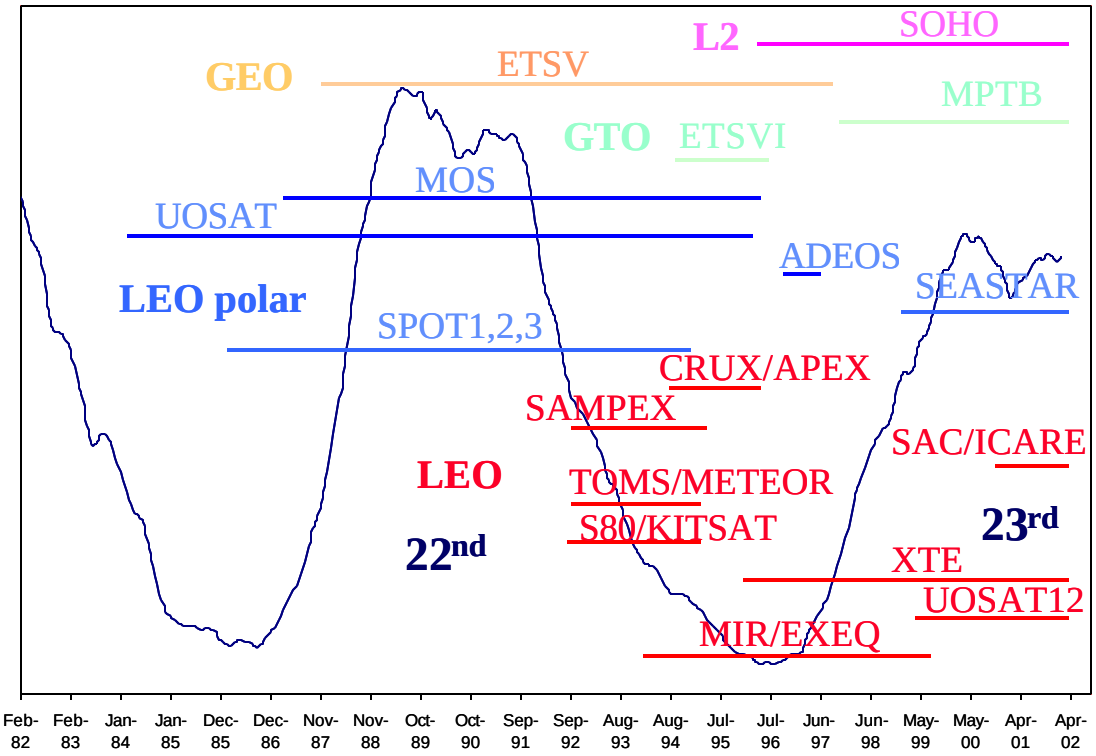

Fig. 1: Period of flight of the different data available. The different orbit types are identified by colors: L2 in magenta, GEO in orange, GTO in green, LEO polar in blue, and other LEO in red. The number of sunspots has also been plotted (black curve) to illustrate the solar activity.

Spacecraft		size	type of memory	part number	manuf.	date		Orbit	data ref.
SOHO	SSR	2Gbit	DRAM 4M*1	SMJ44100	TI	04/01/96	8/30/01	L2	[3]
MOS-1	OBC	1.5Kbit	SRAM 0.5K	93419	FCD	03/01/87	11/30/95	909 km, 99deg	[9]
MOS-1b	OBC	16Kbit	SRAM 4K	CMM5114	RCA	02/07/90	4/25/96	909 km, 99deg	[9]
ETSV	OBC	512Kbit	SRAM64K	uPD4464D-20	NEC	11/24/87	9/12/97	GEO	[9]
ETSVI	OBC	512Kbit	SRAM64K	91901	NEC	09/03/94	6/30/96	8000*38000 km,13 deg	[9]
ADEOS	OBC	1536Kbit	SRAM256K	92001	HIT	09/27/96	6/29/97	800 km, 98.6 deg	[9]
CASSINI	SSR	2*2.5Gbit	DRAM 1M*4		OKI	10/15/97		interplanetary	[52]
SAMPEX	SSR	212 Mbit	SRAM32K*8		HIT	9/5/1992	4/19/95*	580*640 km, 82 deg	[1-2]
TOMS/Meteor3	SSR	128Mbit	SRAM32K*8		HIT	9/5/1992	3/11/95*	1200 km, 82 deg	[1-2]
SEASTAR	SSR	2*512Mbit	DRAM4M*1	MDM1400G-120	HIT	1/1/1999		705 km, 98 deg	[53]
XTE	SSR	512 Mbit	SRAM128K*8	HM628128	HIT	1/1/1996		580 km, 23 deg	[53]
CRUX/APEX	EXP	23Mbit	SRAM128K*8	MT5C1008	MICRON	Aug-94	May-96	362*2544 km, 70 deg	[11-13]
CRUX/APEX	EXP	9Mbit	SRAM128K*8	88130L45PC	EDI	Aug-94	May-96	362*2544 km, 70 deg	[11-13]
CRUX/APEX	EXP	16Mbit	SRAM128K*8	628128	HIT	Aug-94	May-96	362*2544 km, 70 deg	[11-13]
CRUX/APEX	EXP	10Mbit	SRAM32K*8	MT5C2568	MICRON	Aug-94	May-96	362*2544 km, 70 deg	[11-13]
CRUX/APEX	EXP	4.5Mbit	SRAM32K*8	8832C12C1	EDI	Aug-94	May-96	362*2544 km, 70 deg	[11-13]
CRUX/APEX	EXP	4.75Mbit	SRAM32K*8	71256L100DB	IDT	Aug-94	May-96	362*2544 km, 70 deg	[11-13]
APEX	SSR	512 Mbit	DRAM4M*1	HM514100	HIT	8/3/1994	5/16/95*	362*2544 km, 70 deg	[7]
HST	SSR	12Gbit	DRAM4M*4	Luna es rev C	IBM	Feb-97		600 km, 29 deg	[54]
S80T	SSR	96Mbit	SRAM128K*8	D431000	NEC	08/10/92	1995?	1305*1325 km, 66 deg	[3-4-5]
S80T	SSR	8Mbit	SRAM32K*8	D43256	NEC	08/10/92	1995?	1305*1325 km, 66 deg	[3-4-5]
S80T	SSR	8Mbit	SRAM32K*8	CXK58257	Sony	08/10/92	1995?	1305*1325 km, 66 deg	[3-4-5]
KITSAT-1	SSR	96Mbit	SRAM128K*8	CXK58001	Sony	08/10/92	1995?	1305*1325 km, 66 deg	[3-4-5]
KITSAT-1	SSR	8Mbit	SRAM32K*8	CXK58257	Sony	08/10/92	1995?	1305*1325 km, 66 deg	[3-4-5]
UOSAT-5	SSR	8Mbit	SRAM32K*8	D43256	NEC	08/10/92	1995?	770 km, 98 deg	[3-4]
UOSAT-5	SSR	64Mbit	SRAM128K*8	D431000	NEC	08/10/92	1995?	770 km, 98 deg	[3-4]
UOSAT-5	SSR	32Mbit	SRAM128K*8	CXK581000	Sony	08/10/92	1995?	770 km, 98 deg	[3-4]
UOSAT-2	OBC	192Kbit	DRAM16K*1	MKB4116	Mostek	Mar-84		672*654 km, 97.8 deg	[4]
UOSAT-2	OBC	384Kbit	DRAM16K*4	TMS4416	TI	Mar-84		672*654 km, 97.8 deg	[4]
UOSAT-3	SSR	24Mbit	SRAM32K*8	HM62256	HIT	Jan-90		801*782, 98.6 deg	[4]
UOSAT-3	SSR	8Mbit	SRAM32K*8	MSM256	MIT	Jan-90		801*782, 98.6 deg	[4]
FaSat-Bravo	SSR	96Mbit	SRAM128K*8	M5M51008	MIT	Aug-98	Sep-99		[6]
ThaiPhutt	SSR	128Mbit	SRAM512K*8	KMC684000	Samsung	Jul-98	Sep-99		[6]
UOSAT-12	SSR	128Mbit	SRAM512K*8	HM628512	HIT	04/21/99		638*654 km, 64.6 deg	[6]
UOSAT-12	SSR	512Mbit	SRAM512K*8	SYS84000	Samsung	04/21/99		638*654 km, 64.6 deg	[6]
UOSAT-12	SSR	512Mbit	SRAM512K*8	SYS84000	Samsung	04/21/99		638*654 km, 64.6 deg	[6]
SPOT1-2-3	OBC	1.4Mbit	SRAM1K*1	HEF4736	Phillips	Feb-86	1995*	800 km, 97 deg	[10]

Table 1: List of the available flight data on memories (1/2).

Spacecraft		size	type of memory	part number	manuf.	date		Orbit	data ref.
MIR/EXEQ	EXP	3Mbit	SRAM32K*8	HM65756	MHS	Jul-92	Jan-94	350 km, 51.6 deg	[14-15-16]
MIR/EXEQII	EXP	512Kbit	SRAM32K*8	HM65756	MHS	Feb-94	Sep-95	350 km, 51.6 deg	[15-16]
MIR/EXEQII	EXP	2Mbit	SRAM128K*8	MT5C1008	MICRON	Feb-94	Sep-95	350 km, 51.6 deg	[15-16]
MIR/EXEQII	EXP	2Mbit	SRAM128K*8	H68128	HIT	Feb-94	Sep-95	350 km, 51.6 deg	[15-16]
MIR/EXEQII	EXP	32Mbit	DRAM4M4	SMJ416400	TI	Feb-94	Sep-95	350 km, 51.6 deg	[15-16]
MIR/EXEQII	EXP	32Mbit	DRAM16M	Luna E	IBM	Feb-94	Sep-95	350 km, 51.6 deg	[15-16]
MIR/EXEQIII	EXP	512Kbit	SRAM32K*8	HM65756	MHS	Oct-95	Mar-97	350 km, 51.6 deg	[15-16]
MIR/EXEQIII	EXP	2Mbit	SRAM128K*8	MT5C1008		Oct-95	Mar-97	350 km, 51.6 deg	[15-16]
MIR/EXEQIII	EXP	128Kbit	SRAM64K		russian	Oct-95	Mar-97	350 km, 51.6 deg	[15-16]
MIR/EXEQIII	EXP	32Mbit	DRAM4M4	SMJ416400	TI	Oct-95	Mar-97	350 km, 51.6 deg	[15-16]
MIR/EXEQIII	EXP	64Mbit	DRAM64M	IBM50G6269	IBM	Oct-95	Mar-97	350 km, 51.6 deg	[15-16]
MIR/EXEQIV	EXP	1Mbit	SRAM128K*8	MT5C1008	MICRON	Jul-98	Aug-99	350 km, 51.6 deg	[16]
MIR/EXEQIV	EXP	8Mbit	SRAM512K*8	HM628512	HIT	Jul-98	Aug-99	350 km, 51.6 deg	[16]
MIR/EXEQIV	EXP	8Mbit	SRAM512K*8	M5M5408		Jul-98	Aug-99	350 km, 51.6 deg	[16]
MIR/EXEQIV	EXP	8Mbit	SRAM512K*8	KMC684000	Samsung	Jul-98	Aug-99	350 km, 51.6 deg	[16]
MIR/EXEQIV	EXP	8Mbit	DRAM1M4	EDI441024		Jul-98	Aug-99	350 km, 51.6 deg	[16]
MIR/EXEQIV	EXP	32Mbit	DRAM4M4	SMJ416400	TI	Jul-98	Aug-99	350 km, 51.6 deg	[16]
SAC_C/ICARE	EXP	32Mbit	DRAM4M4	SMJ416400	TI	Nov-00	Jun-02	707km, 98.2 deg	[22]
SAC_C/ICARE	EXP	512Mbit	DRAM16M*4-3.3V	KM44V16004	Samsung	Nov-00	Jun-02	707km, 98.2 deg	[22]
SAC_C/ICARE	EXP	256Mbit	DRAM16M*4-3.3V	HM516405	HIT	Nov-00	Jun-02	707km, 98.2 deg	[22]
SAC_C/ICARE	EXP	128Mbit	DRAM8M8	0165805	IBM	Nov-00	Jun-02	707km, 98.2 deg	[22]
SAC_C/ICARE	EXP	24Mbit	SRAM512K*8	HM628512	HIT	Nov-00	Jun-02	707km, 98.2 deg	[22]
SAC_C/ICARE	EXP	24Mbit	SRAM512K*8-3.3V	KM684000	Samsung	Nov-00	Jun-02	707km, 98.2 deg	[22]
SAC_C/ICARE	EXP	256Kbit	SRAM32K*8	HM65656	MHS	Nov-00	Jun-02	707km, 98.2 deg	[22]
MPTB/neural b.	EXP	256Kbit	SRAM32K*8	HM62256	HIT	Apr-98	Apr-02	1220*39200km,63.6 deg	[17-18]
MPTB/neural b.	EXP	256Kbit	SRAM32K*8	HM65756	MHS	Apr-98	Apr-02	1220*39200km,63.6 deg	[17-18]
MPTB/DRAM b.	EXP	1Gbit	DRAM4M4	uPD4217800	NEC	Nov-97	8/1/99*	1220*39200km,63.6 deg	[19-20]
MPTB/DPRAM b.	EXP	2Mbit	SRAM32K*8	M65656	MHS	Mar-98	Mar-99	1220*39200km,63.6 deg	[21]
MPTB/DPRAM b.	EXP	1Mbit	DPRAM16K*8	7006	IDT	Mar-98	Mar-99	1220*39200km,63.6 deg	[21]
MPTB/DPRAM b.	EXP	1Mbit	DPRAM8K*16	70V25	IDT	Mar-98	Mar-99	1220*39200km,63.6 deg	[21]

Table 1: List of the available flight data on memories (2/2).

Both SRAMs and DRAMs have been flown, the latest experiments fly 4M SRAMs and 64M DRAMs. Only a few information is available on EEPROMs. No flight data has been published on flash EPROMs and SDRAMs.

2.2 trends observed (summary)

2.2.1 Spatial Location of upset, daily and orbital variation of the upset rates

Most of the data available is on parts that are sensitive to both heavy ion and proton induced upsets. All the data available for all orbits exposed to trapped protons show a high correlation with proton flux contours of standard AP8 models. LEO orbits with high inclination are exposed to GCR and Solar particles in the high latitude regions of the orbit. Low altitude (< 500 km), low inclination (<30 degrees) orbits show a little exposition to GCR and solar particles.

2.2.1.1 Example 1: SEASTAR, LEO polar orbit

Fig. 2 shows the location of upsets accumulated from January 1999 to June 2002 on the SEASTAR spacecraft. We see a high density of trapped proton induced upsets in the SAA, the GCR and solar particle induced upsets are located on high latitude regions of the orbit.

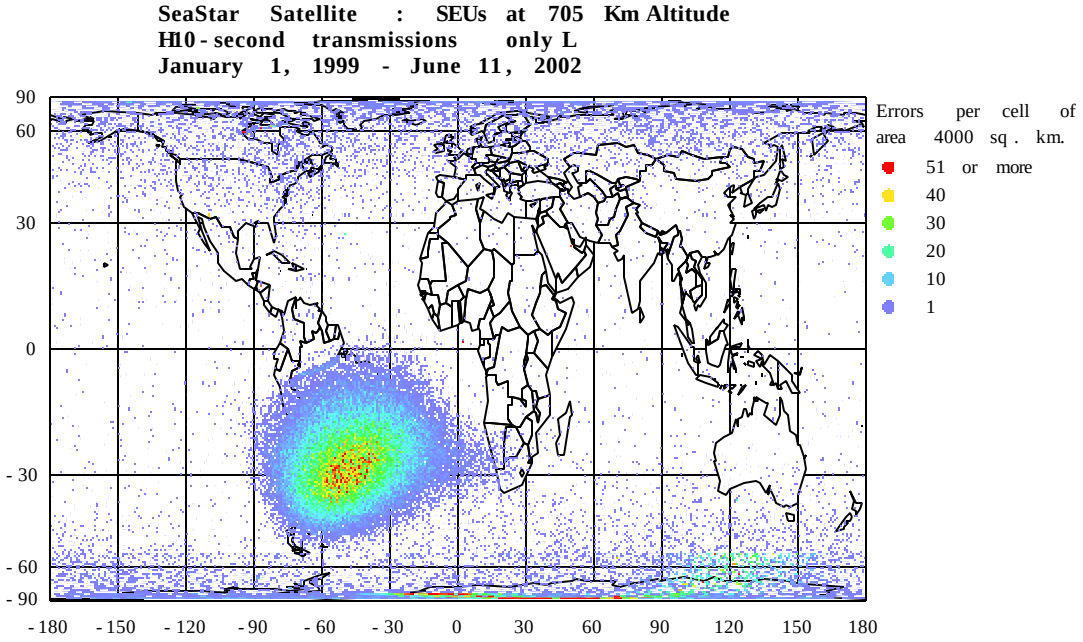

Fig 2: SEU density plot on SEASTAR FDRS from January 1999 to June 2002.

Fig 3 shows the location of the upsets during a typical day (July 13, 2000). More than 80% of the SEUs occur in the SAA and the other are induced by the Galactic Cosmic Rays in the high latitude regions. We can see that the upsets appear in bursts because 80% of the upsets occur in the SAA where the spacecraft spends only 5% of its time. Fig 4 shows the location of the SEU on July 13 and July 14, 2000. In July 14, 2000 we observed one of the main solar events of the current solar cycle. We can see in Figure 4 that the number of SEU that occur in the SAA is similar for the two days, but the number of SEU in the high latitude regions is significantly higher on July 14, 2000.

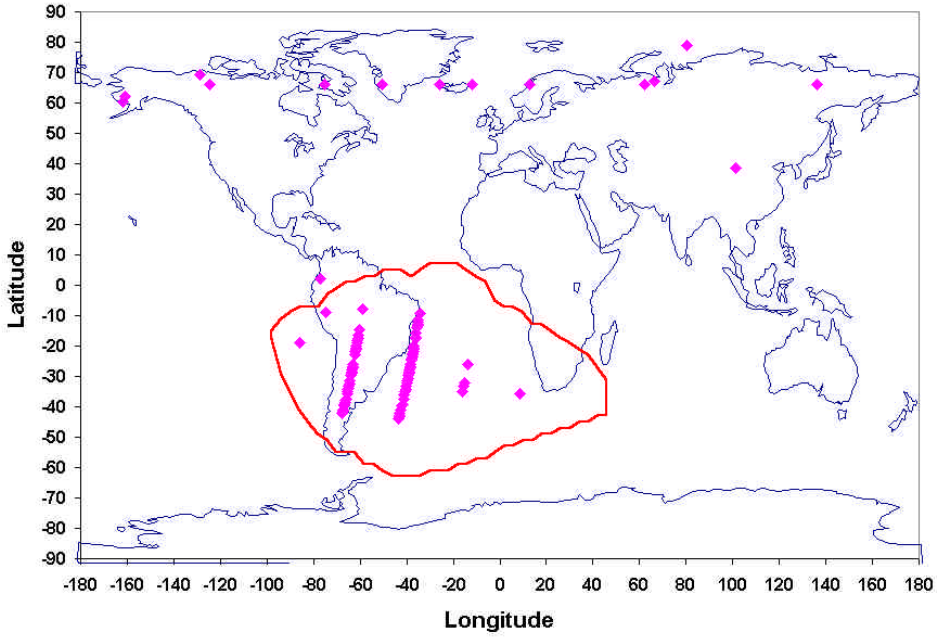

Fig 3: SEASTAR FDR, SEU location on a typical day (July 13, 2000).

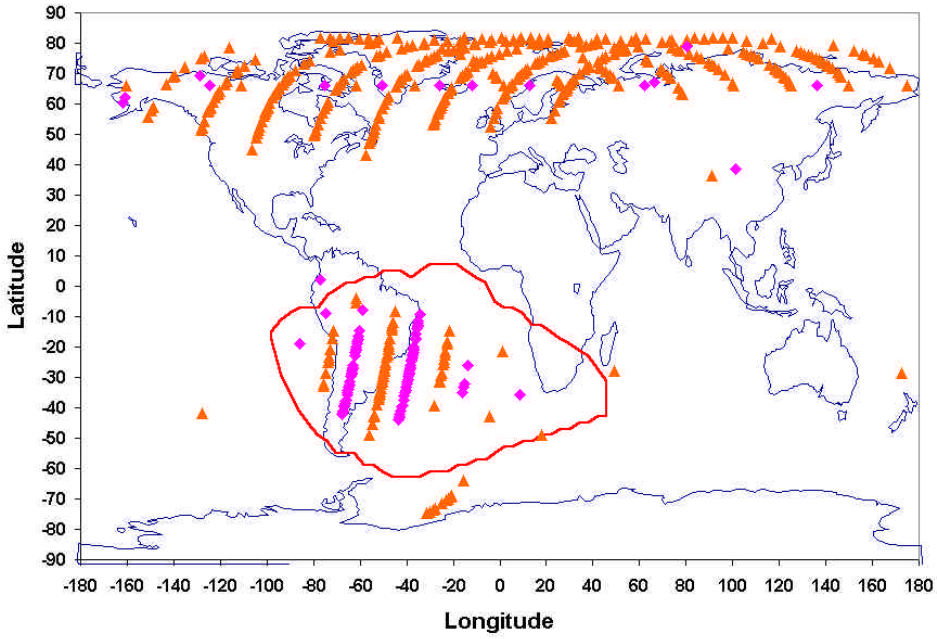

Fig. 4: SEASTAR FDR location of SEU on July 13 (in magenta) and July 14, 2000 (in orange).

2.2.1.2 Example 2: LEO elliptical orbit APEX/CRUX experiment

APEX orbit with of perigee of 362 km and an apogee of 2544km with an inclination of 70 degrees allowed a mapping of the upset rates in nearly the whole trapped proton belt [11-13]. The SEU rates in the trapped protons belts vary significantly with the altitude as shown in Fig 5 to 7. These figures show the 1M SRAM HITACHI 628128 SEU rates and location for different altitude ranges.

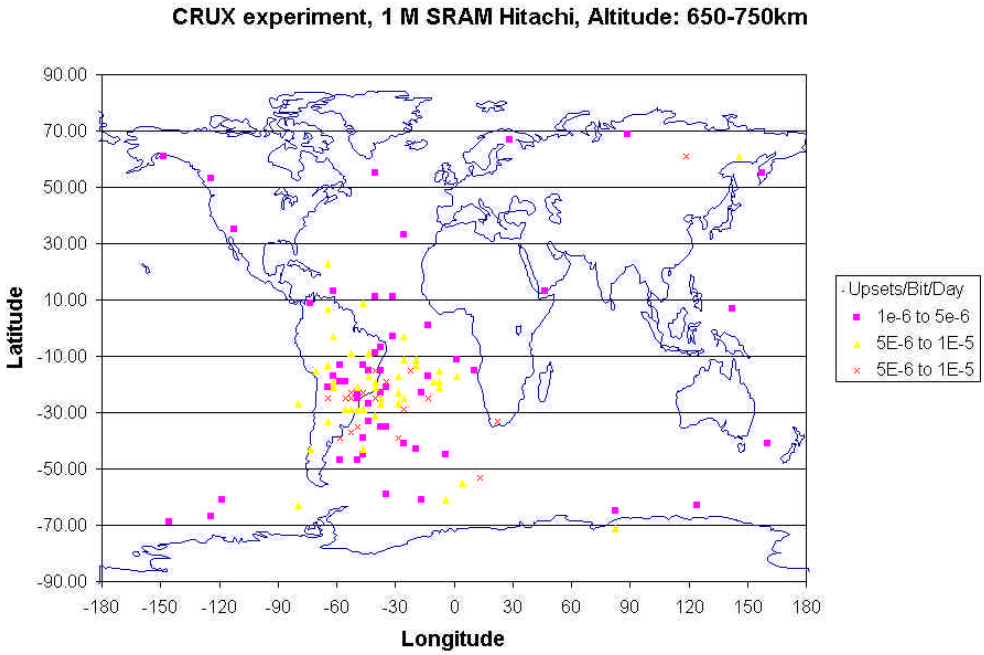

Fig 5: CRUX experiment SEU location and upset rates for the 1M SRAM HITACHI 628128 and the 650 km to 750 km altitude range.

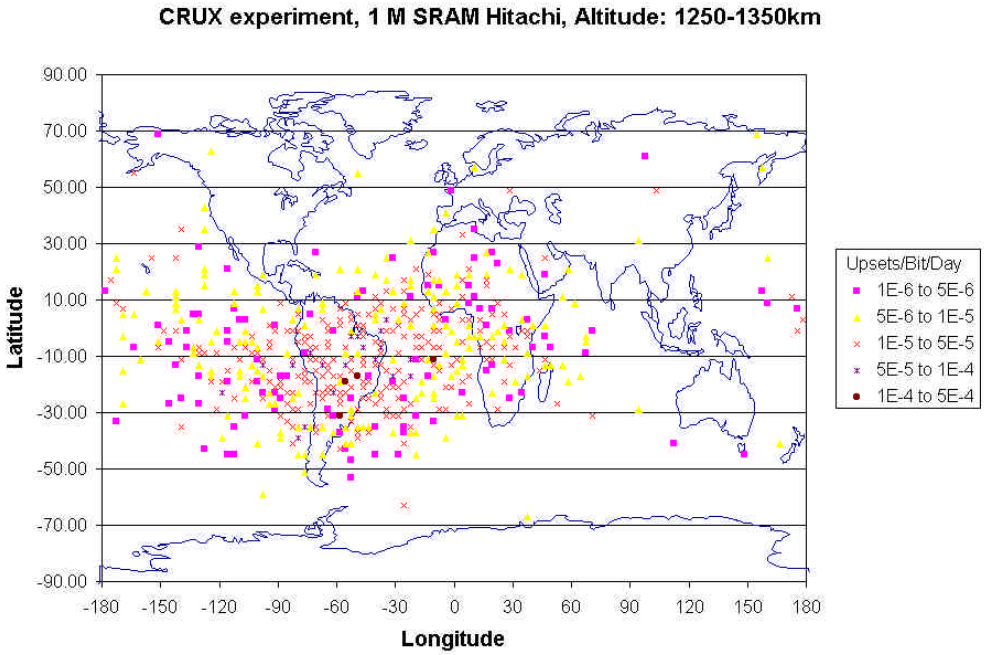

Fig 6: CRUX experiment SEU location and upset rates for the 1M SRAM HITACHI 628128 and the 1250 km to 1350 km altitude range.

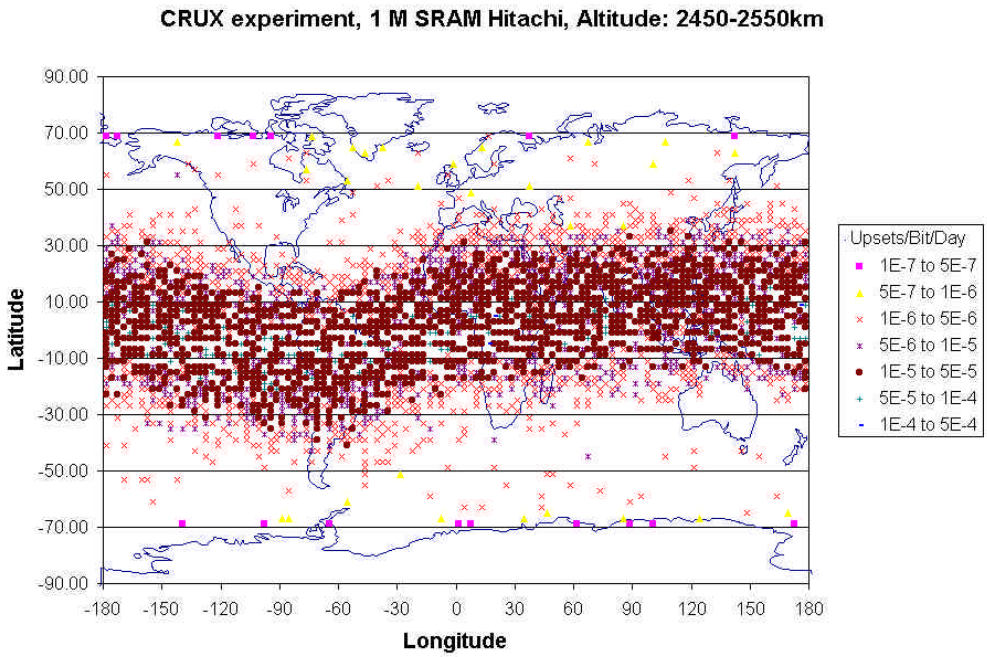

Fig 7: CRUX experiment SEU location and upset rates for the 1M SRAM HITACHI 628128 and the 2450 km to 2550 km altitude range.

The upset rates at all altitudes show a high correlation with proton flux contours of the standard model AP8. At 700 km, the trapped protons induced SEU are located in the SAA. Then the SEU contours extend with the increasing altitude.
The effect of altitude on SEU rates can be clearly seen from these figures. At 1300 km the SEU rates are eight to eleven times higher than at 700 km. At 2500 km, they are twenty to thirty times higher. The 2500 km altitude is close to the peak of the proton population.

2.2.1.3 Example 3: LEO low altitude, low inclination, XTE

XTE is a LEO 573 km altitude, 23 degrees inclination orbit. XTE spacecraft is losing altitude with time. In Fig. 8 the monthly average of the number of SEU/day and the spacecraft altitude are plotted for the period from July 1996 to July 2002. XTE spacecraft is losing altitude with time. We can see in Fig. 8 the decrease of the upset rates with the decreasing altitude. In July 1996, the spacecraft altitude is about 573 km and the average SEU rate is 250 SEU/day. In July 2002, the spacecraft altitude has decreased to about 520 km, and the average SEU rate is 70 SEU/day.
This data illustrate the large variation of the trapped proton fluxes, and therefore the SEU rates, with the altitude in this low altitude range.

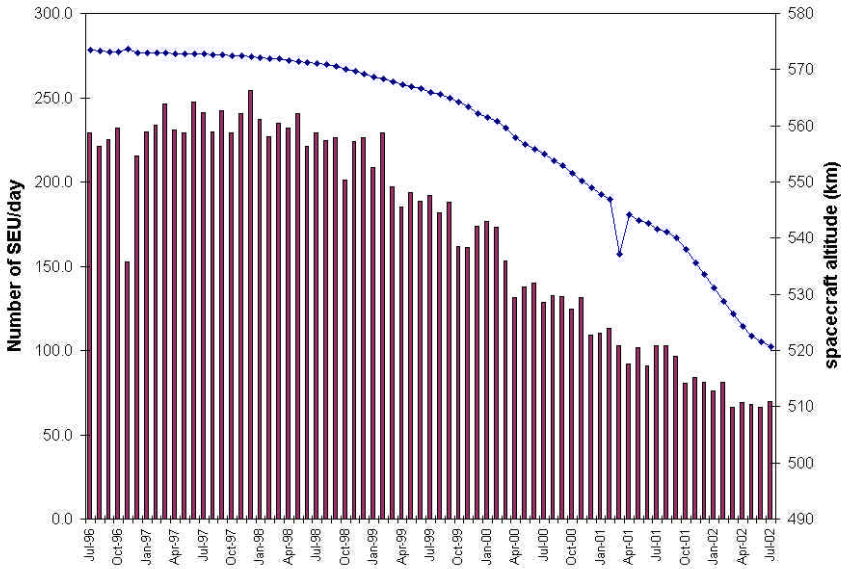

Fig. 8: XTE SSR flight data, plot of the monthly average of the number of SEU/day, and of the spacecraft altitude versus time from July 1996 to July 2002.

2.2.2 Effect of space weather on the SEU rates

2.2.2.1 Solar Events

Solar Particle Events (SPE) may have a significant impact on the upset rates.
A high sensitivity to high-energy solar particles have been observed on all spacecraft exposed to the solar particles during solar max activity. The impact of SPE varies with the exposition to the solar particles (type of orbit and shielding) and also the type of device.

- LEO polar or high inclination orbits: SAC/ICARE [22], UOSAT [3-4], SAMPEX [1-2], MOSI [9], SEASTAR [53]
- GTO: MPTB [18,20]
- GEO: ETSV [9]
- L2:SOHO [3]

No sensitivity to SPE was reported on

- low altitude low inclination orbits: MIR [14-16], XTE [53]

As an example Fig. 9 shows the daily SEU counts on SEASTAR SSR from January 1999 to June 2002. We can see that 5 solar events have induced an increased SEU number on the SEASTAR SSRs. Other solar events have been observed during this period but only the events with a significant increase of high energy protons (>60-100 MeV) have induced increased SEU rates on SEASTAR SSRs.

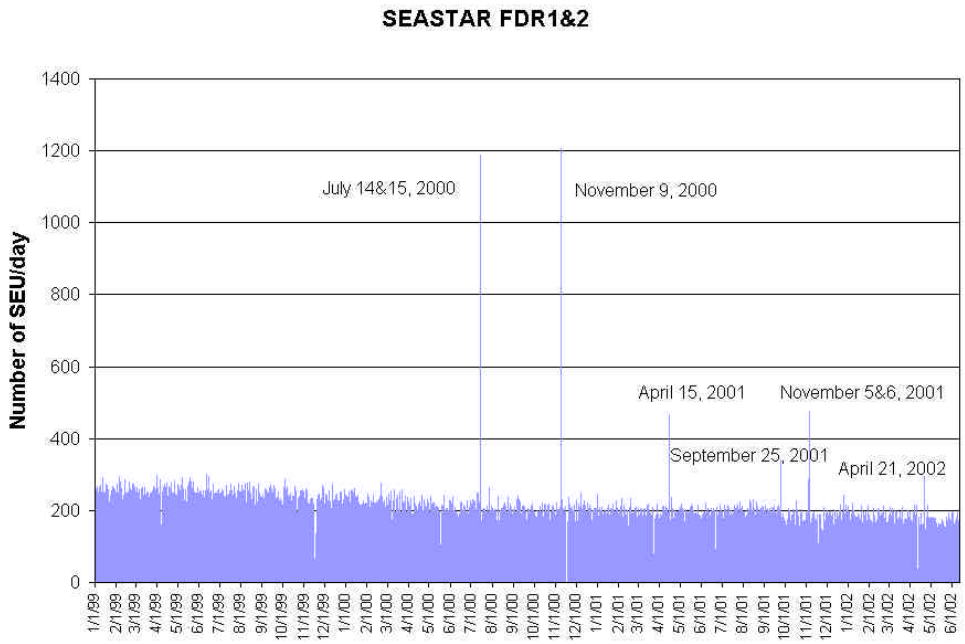

Fig. 9: Daily SEU rates on SEASTAR SSR from January 1999 to June 2002.

Fig. 10 shows the proton spectrum composition of these 5 solar events (July 14 2000, November 9 2000, April 15 2001, September 25 2001, and November 5 2001) as given by the measurement from the GOES spacecraft. Fig. 11 plots the SEU rates and the >100 MeV proton fluxes these days. We can see a good correlation of the SEU rates with the >100MeV proton fluxes.

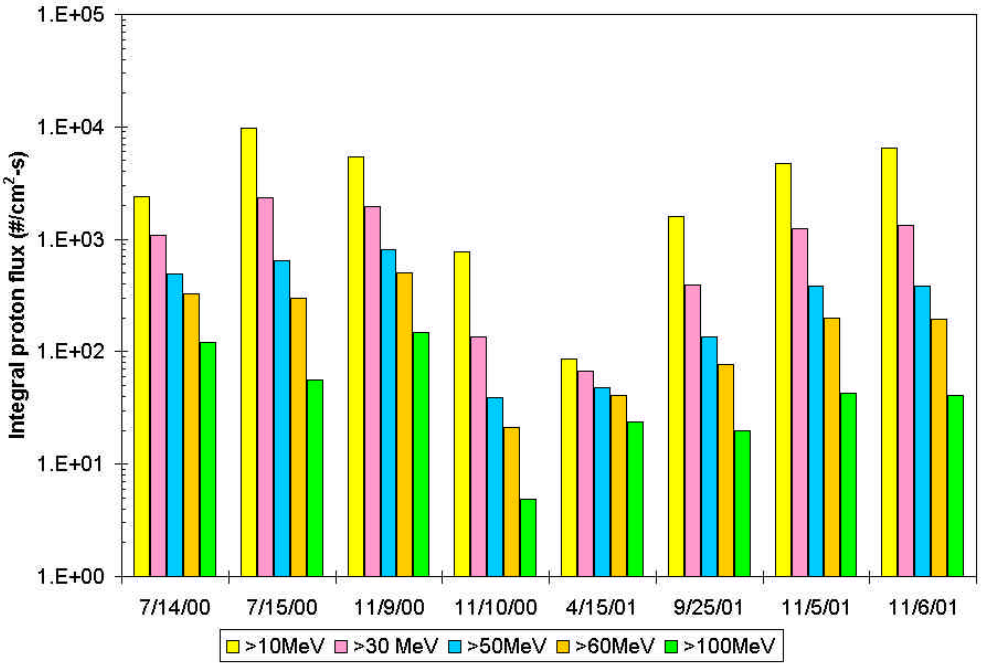

Fig. 10: Proton Spectrum composition of the main solar events of the current solar cycle.

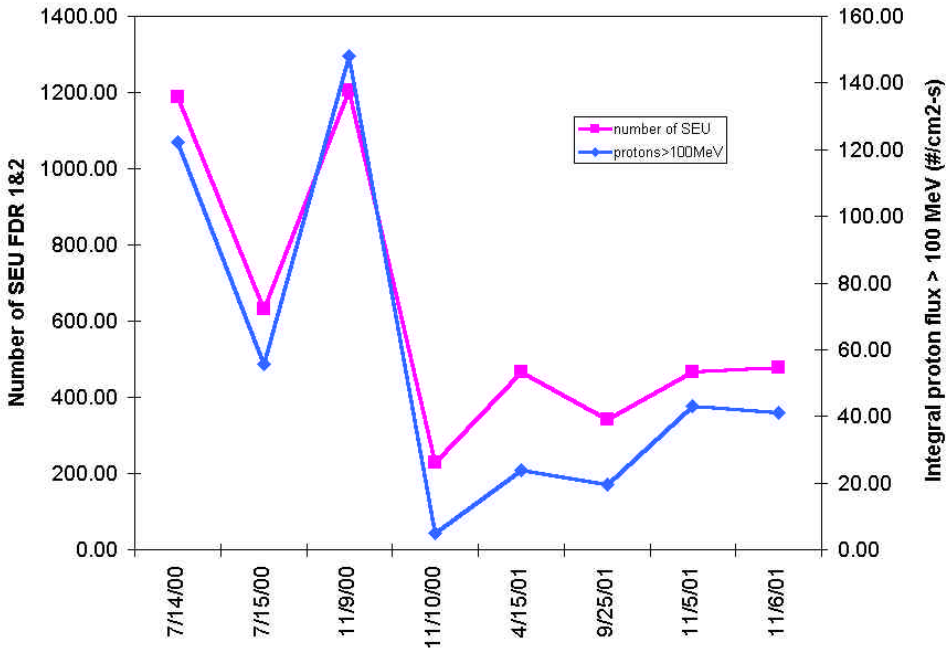

Fig. 11: SEU rates on SEASTAR SSRs and solar proton >100 MeV fluxes during the main solar events of the current solar cycle.

SAC/ICARE flight data has also shown a correlation of the SEU rates during a SPE with the >80 MeV proton fluxes [22]. This illustrates the fact that the solar proton spectrum is much softer than the GCR proton spectrum and therefore an accurate shielding analysis is important to predict accurately the SEU rates during a SPE.

2.2.2.2 Solar cycle modulation

In agreement with the environment models, the data collected on a sufficient number of parts and a sufficient duration shows the modulation of the particle fluxes (GCR and trapped protons) and therefore the SEU rates with the solar activity.

Fig. 12 shows the monthly averages of the daily SEU rates observed on the SEASTAR SSRs and the smoothed sunspot numbers that give an idea of the solar activity. We can see, as expected, the decreasing SEU rates with the increasing solar activity. Another example of the modulation of the trapped proton fluxes is shown in the MOS1 data for the previous solar cycle (cycle 22) [9].

SOHO data [3] illustrates the modulation of the GCR background, with a decline of the SEU rates as solar maximum approaches (solar cycle 23).

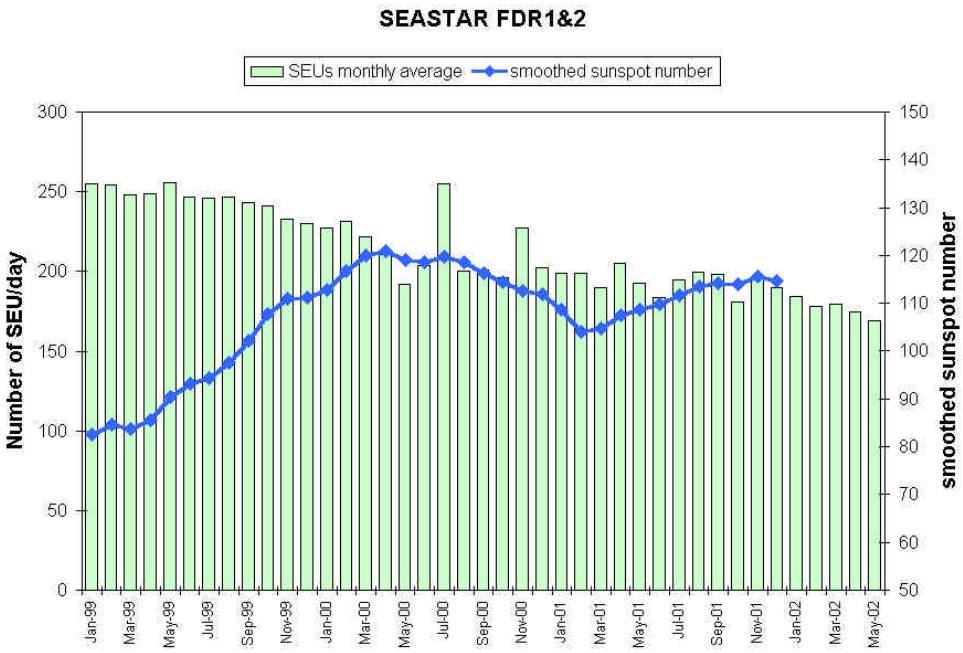

Fig. 12: Monthly averages of the daily SEU rates on SEASTAR SSRs and smoothed sunspot numbers.

2.2.3 Other SEU observations

2.2.3.1 Part to part dispersion

Large part to part dispersion of the SEU sensitivity (up to a factor 12) has been observed on several experiments (CRUX/APEX, KITSAT, MIR/EXEQ, MIR/EXEQIII). Main factor is the actual part to part dispersion as shown by the CRUX analysis [12, 13] and the retest of flight part of MIR/EXEQ flight parts [15, 16]. This illustrates the poor fidelity of a test on 2 or 3 parts.
Another factor that may impact the SEU sensitivity is the exposition to the radiation environment (shielding) [12,13].

2.2.3.2 Pattern sensitivity

Flight data of memory experiments has shown that SRAM cells can have a different SEU sensitivity depending of the cell programmed state. The worst case was observed on the CRUX experiment for the MICRON 1M SRAM where 98% of SEU were bit flips from 1 to 0, and only 2% of SEU were bit flips from 0 to 1. Other devices did not show any effect of the programmed logic state, like the EDI SRAM [11-13]. This pattern sensitivity is easily detected during ground testing.
DRAM cells can only be upset when the cell capacitor in is the charged state. The charged state for some cells corresponds to a logic level of 1 and for other cells it corresponds to a logic level of 0. Because of this a memory cell has only bit flip from 1 to 0 when the charged state corresponds to a logic level of 1, and bit flip from 0 to 1 in the other case. Generally half of the memory bits are at a logic level of 1 and the other half at a logic level 0 when the capacitor is charged. In this case no pattern dependence is observed with standard tests pattern. If this is not the case, like in the 4Mbit DRAM from TI, both flight and ground test data show a strong pattern dependence [15].

2.2.4 Other radiation effects

2.2.4.1 MBU

Generally for SSR and OBC memories, only the critical MBUs (for example the Single word Multiple bit Upset, SMU) that caused an uncorrectable error can be identified. On memory experiments because of the fast scrubbing rates, it is generally possible to identify the MBU, and their size [14-19, 22]. When the memory mapping was known, it has also been possible to identify the mechanism that caused the MBU. In the MPTB DRAM experiment, MBU caused by ions impacting a memory device at grazing incidence, and MBU row errors caused by an ion impact in the memory control circuitry have been clearly identified [19]. This MBU flight data is extremely important because it is often very difficult to analyze the ground test data (because of the accelerated flux) and or simulate the space environment during ground testing (for example the effect of ions at grazing incidence).

The ratio MBU versus SEU varies from about 1% to 20% depending on the device type and orbits. As expected, DRAMs are more prone to MBU than SRAMs. The more recent memories (4M SRAM, 16M and 64M DRAM) do not show an increased MBU sensitivity. The most sensitive MBU device is the SMJ416400 16M DRAM from Texas Instruments with a ratio MBU versus SEU of about 20% [15,16,22]. On 64M DRAMs this ratio varies from 2 to 10% [22]. The ratio MBU versus SEU of the 1M SRAM MT5C1008 from MICRON is about 10%, It is less than 5% on three different types of 4M SRAMs [16,22]. However ground test data shows that the percentage of SMU (that may cause critical errors in systems) seems more important in recent memories [25]. The flight data does not seem to confirm this but statistics is very low.

All flight data show that proton can induce MBU, but the largest clusters of upsets and the highest ratio MBU versus SEU is obtained with heavy ions. For example on the MPTB DRAM experiment, the ratio MBU versus SEU is about 20% outside the proton belts, it is about 8% inside the proton belts and most of the MBU are double bit upsets [19].

2.2.4.2 SEFI

Sometimes, MBU block errors can not be cleared by rewriting the locations with new data; they are cleared by cycling the power or resetting the device. This type of error may be viewed as a type of SEFI. This type of event has been observed in flight on the Hubble Space Telescope (HST) SSR. This error has been attributed to a proton-induced error in the internal redundancy latch of each DRAM memory device [54]. This sensitivity was identified during preflight heavy ion testing, but proton testing did not show any sensitivity. Therefore the SEFI problem was considered as a non issue for the HST mission.

Further proton testing on a large number of devices (100 parts) was performed after the anomaly was detected in flight. The results showed SEFI block errors, and the predicted rates based on the measured cross section and the HST environment were within the same order of magnitude as the observed in-flight rate. This is another interesting example of the poor fidelity of a test on 3 devices for a system that uses 1440 devices.

2.2.4.3 SHE

Stuck bits were reported on SRAM 256K and 1M devices on the CRUX/APEX [11-13], and the MPTB neural board experiments [17,18]. The stuck bits resume normal operations on their own after a period of time ranging from minutes to several months [11-13, 17, 18]. On MPTB, bursts of stuck bits were observed during some solar particle events (November 1998, November 2001). On MPTB the Stuck bit rate has also increased with the increased time, and then the increasing dose [18]. All these observation lead us to the conclusion that these stuck bits are due to micro dose effect mainly induced by heavy ions. No SEGR has been identified in flight.

Other experiments, using SHE sensitive devices, did not show any in flight sensitivity [3,4,5]. Ground testing data has shown that more recent SRAM and DRAM are less sensitive to SHE. This is confirmed by the flight data [6, 22].

2.2.4.4 SEL

SEL are reported on the 64K SRAM uPD4464 from NEC on the ETSV spacecraft [9]. 2439 SEL during about 10 years have been observed. SEL ground testing showed this extremely high sensitivity of this part with a SEL LET threshold less than 1 MeVcm^2/mg.. The SEL rates were calculated with CREME96 assuming a shielding thickness of 21mm Al, and a worst case thickness of the sensitive volume of 1 µm. The predictions overestimate the flight rates by a factor 4 for the background environment. The predictions give accurate estimations of the SEL rates during the solar events with the CREME96 worst week and worst day solar event models.
A proton induced SEL has been reported on the same memory device on an instrument of the ERS-1 satellite [26].
One possible occurrence has been reported on a 256K SRAM from IDT on the CRUX experiment. SEL were observed on this part during ground tests [12-13].
No other SEL occurrence has been observed.

2.2.4.5 TID

No TID induced failure has been reported. After 10 krad accumulated on the S80 SSR, the 5V current has doubled [3-5]. On MPTB the stuck bit rate has also increased with the increased time, and then the increasing dose [18].

2.2.5 Comparison of SEU rates with prediction

2.2.5.1 Introduction

Significant uncertainties are involved in SEU rate prediction:
- The uncertainty in the radiation environment (radiation models and shielding assumptions)
- The uncertainty in the SEU characterization.
- The uncertainty in the sensitive volume thickness.

Considered these large uncertainties in this calculation, it is generally considered that an accurately calculated SEU rates predict the average flight rates over a long period of time within one order of magnitude. Because of the conservative assumptions that are made for these calculations, the calculated rates generally overestimate the actual flight rates, but it is not always the case. In 13 cases out of the 53 cases analyzed, the SEU rates have been underestimated.

2.2.5.2 SRAMS

Generally the event rates predict the flight rate within a factor 5. In some cases large overestimations are observed:
- Proton rate predictions: a factor 55 overestimation on the 256K SRAM from EDI on CRUX, a factor 6 overestimation on the 256K SRAM from IDT on CRUX [11-13], and a factor 15 overestimation on the 256K SRAM from Sony on S80 [3-5] is reported. In these three cases only partial proton test data was available (only one data point for CRUX memories) and a Bendel fit has been used to calculate the upset rate. This shows the importance to take proton test data in addition to heavy ion test data. Inaccurate shielding thickness assumptions may have also played a role in these large overestimations.
- Heavy ion rate predictions: a factor 10 overestimation on the 256K SRAM from Micron, and a factor 100 overestimation on the 256K SRAM from EDI is reported on CRUX data [11-13]. Flight data on show a factor 12 device to device variation in the SEU rates on EDI 256K SRAM, a factor 2 on Micron 256K SRAM, and both devices exhibit significant pattern sensitivity. In addition test data has not been taken on the flight lots. Poor test fidelity seems to be the main cause of these discrepancies.

Table 2 lists the cases where the calculated rates underestimate the actual flight rates. In all but 2 cases, the predictions are within about a factor 5 with the flight rates. Three different missions are concerned: S80, KITSAT, and MIR/EXEQIV. For these three missions most of the predictions are underestimated. On S80 and KITSAT, trapped protons dominate the radiation environment. One possible cause of these underestimation is an overestimation of shielding thickness. But in the two large cases of underestimation (CXK58001 on KITSAT, CXK58257 on S80) an inaccurate SEU characterization is suspected. Flight data on the CXK58001 show a factor 10 device per device variability. On MIR/EXEQIV, either protons or heavy ions dominate the part response depending on the part type. For proton dominated responses, possible causes of these underestimation are an overestimation of the shielding thickness, and/or an underestimation of the proton fluxes at low altitude by the AP8 solar maximum model [55]. For heavy ion dominated responses, a possible cause of the underestimation is the use of the old CREME model, with the weather index M=1 (average flux) at solar maximum.

Mission	Manufacturer	Function	Device type	Solar activity	ratio predicted/ observed	predominant source of SEU	Comments
S80T/SSR	NEC	SRAM128K*8	D431000	solmin	0.37	protons	protons prediction only
S80T/SSR	Sony	SRAM32K*8	CXK58257	solmin	0.14	protons	protons prediction only
S80T/OBC	Sony	SRAM128K*8	*CXK51000*	solmin	0.25	protons	protons prediction only
KITSAT-1/SSR	Sony	SRAM128K*8	CXK58001	solmin	0.07	protons	protons prediction only; 10:1 device/device variability
KITSAT-1/OBC	Sony	SRAM128K*8	CXK581000	solmin	0.22	protons	protons prediction only
UOSAT-5/SSR	NEC	SRAM128K*8	D431000	solmin	0.21	protons	protons prediction only
MIR/EXEQIV	MICRON	SRAM128K*8	MT5C1008	solmax	0.59	heavy ions	
MIR/EXEQIV	HIT	SRAM512K*8	HM628512	solmax	0.17	heavy ions	
MIR/EXEQIV		SRAM512K*8	M5M5408	solmax	0.63	heavy ions	
MIR/EXEQIV	Samsung	SRAM512K*8	KMC684000	solmax	0.19	protons	

Table 2: list of the cases where the calculated SEU rates underestimate the actual flight rates.

2.2.5.3 DRAMS

Fewer data is available to compare DRAM flight upsets rates to predictions. We have this information for:

- SOHO SSR [3] and MIR/EXEQ [16] where the heavy ion induced upsets are dominant
- MPTB DRAM experiment [19, 20] and APEX SSR [7] where the proton induced upsets are dominant.

Proton rates predictions give an estimation of the flight rate within a factor 2 [7,20]. In both cases proton test data was available for at least three energy points.

Heavy ion rates give an estimation of the flight rates within a factor 5. But larger discrepancies were reported when the assumption of the sensitive volume (SV) thickness was too conservative. For example, for the 16M DRAM flown on MIR/EXEQ the calculated rate overestimates the actual flight rate by a factor up to 45 when a 2µm thickness of SV is assumed. When a more realistic thickness of SV is assumed (7 µm), the overestimation is reduced to a factor 4 [16]. If the conservative assumption of a "standard" SV thickness of 2 um works well for SRAMs, it may be too conservative for deep SV of DRAMs.

Table 3 lists the cases where the calculated rates underestimate the actual flight rates. In all cases, the predictions are within about a factor 5 with the flight rates. Like for SRAMs flying in the same missions, the main cause of the underestimation is possibly the environment models (proton and heavy ions) and the shielding assumptions. In addition, for the 64M DRAM IBM50G6269 flown flown on MIR/EXEQIII, the flight data statistics is too low to draw definitive conclusions.

Mission	Manufacturer	Function	Device type	Solar activity	ratio predicted/ observed	predominant source of SEU	Comments
MIR/EXEQIII	IBM	DRAM64M	IBM50G6269	solmin	0.34	protons	low flight data statistics (2 events)
MIR/EXEQIV	EDI	DRAM1M4	EDI441024	solmax	0.30	heavy ions	
MIR/EXEQIV	TI	DRAM4M4	SMJ416400	solmax	0.65	heavy ions	

Table 3: list of the cases where the calculated SEU rates underestimate the actual flight rates.

2.2.5.4 Prediction of SEU rates during SPE

Comparison of calculated rates with actual rates during SPE has only been done for SOHO SSR [8] and MPTB DRAM experiment [20]. Orders of magnitude overestimations of the July 14, 2000 event upset rates are reported when the CREME96 solar event environment models were used.
In both cases the background environment rate has been predicted within a factor 2. The proton spectrum of CREME96 model is based on October 89 solar event and is similar to proton spectrum of July 14, 2000 solar event. One possible explanation is the difference in the heavy ion LET spectrum as shown in Fig 13 that compares the CREDO measurements on MPTB [56] to the CREME96 worst day model LET spectrum. Rates calculated with this measured spectrum are in good agreement with the observed rate on MPTB during the July 14 solar event [20].

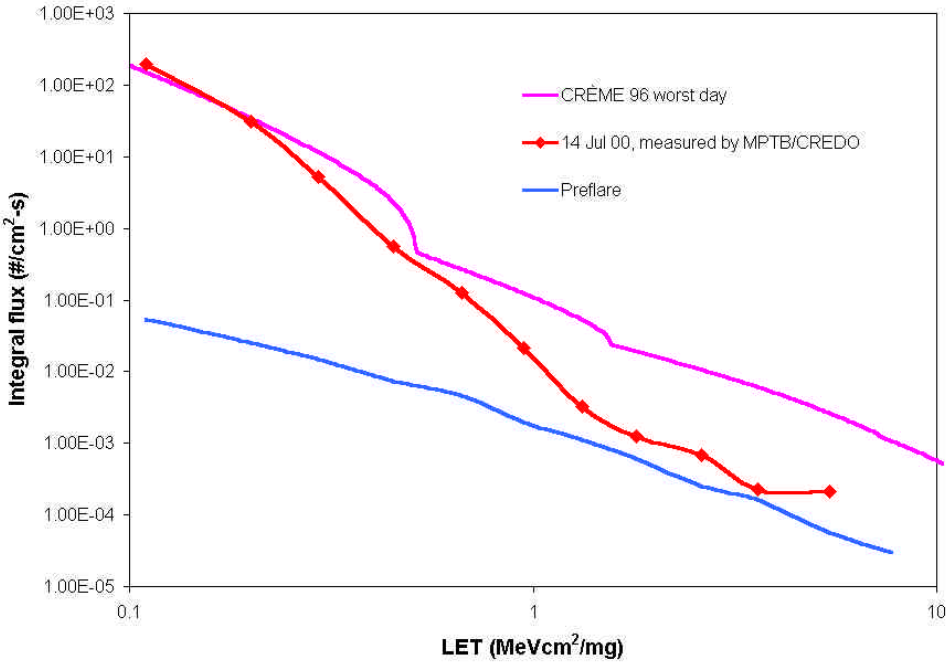

Fig 13: Comparison of the CREME96 worst day model LET spectrum with the measured LET spectrum on CREDO-3/MPTB on July 14, 2000.

Another cause of error during a solar flare is an inaccurate estimation of the shielding. Generally upset rates are calculated for a conservative value of shielding (100 mils, 1g/cm^2 of Al). This is often sufficient to calculate GCR and trapped protons induced SEU rates, but this could lead to large errors in the calculation of solar particle induced SEU rates, because of the "softer" solar particle spectra. SEASTAR analysis (see Fig 11) shows that only high-energy protons (>80 MeV) create an increased SEU rate; the same conclusion has been done on SAC/ICARE experiment [22]. The MPTB prediction that gives a good agreement with July 14, 2000 event rates has been made with a reasonably accurate model of the shielding.

3 Mitigation techniques utilized

Error Detection and Correction (EDAC) coding schemes are used to protect the memories from the SEU. The memories are regularly scrubbed to prevent the accumulation of bit errors due to SEUs. Their content is read through the EDAC protection circuitry (to correct the errors) and written back, such that the corrected data are restored on a regular cyclical basis. Table 4 lists the different types of codes used in the data analyzed here.

Spacecraft	Subsystem	EDAC code	Data word size (bits)	# code bits	Scrubbing rate (minutes)
SEASTAR	SSR	Hamming	8	4	
SOHO	SSR				29
S80T	OBC				8.5
KITSAT-1	OBC				8.5
UOSAT-5	OBC				8.5
UOSAT-2	OBC				
APEX	SSR		16	6	4
CASSINI	SSR		32	7	
SAMPEX	SSR				5
XTE	SSR				25
TOMS	SSR		64	8	0.27
FaSat-Bravo	OBC	TMR	8	16	13
Thai Phutt	OBC				13
UOSAT-12	OBC				13
S80T	SSR	Reed Solomon	252x8	3 x8	222
KITSAT-1	SSR				222
UOSAT-5	SSR				222
UOSAT-3	SSR				222
FaSat-Bravo	SSR				
Thai Phutt	SSR				
UOSAT-12	SSR1				
UOSAT-12	SSR2		252x8	4 x8	
HST	SSR		224x8	31 x8	32

Table 4: EDAC techniques used.

One of the most popular EDAC code is the Hamming code. This code is able to detect and correct any single-bit error, and to detect double bit errors in a data word. This simple technique has proved its effectiveness as long as a single particle does not cause multiple errors in a data structure, and the scrubbing rate is adequate to avoid coincidental but independent events in a data word. When this occurs the failure rate is virtually negligible. Two occurrences of high uncorrectable SEU rates have been reported. On the CASSINI SSR an unexpectedly high rate of uncorrectable double bit errors has been observed [52]. About two uncorrectable errors per day are observed, while virtually none were expected. An analysis has shown that these uncorrectable errors were due to the unusual architecture: one data word of 39 bits is stored in two passes in the 20 bits wide memory architecture made with five 1Mx4 DRAMs. The second pass for word accesses the very next 4 bit segment in each DRAM device. Unfortunately, each bit in the second segment is physically adjacent to the corresponding bit in the first segment. Thus MBU can corrupt 2 bits in the 39 bit word. This example shows that designers of space systems need to carefully consider how parts are being used in system architectures. Fig 14 shows the number of uncorrectable errors that have occured on the XTE SSR [53]. The rate is low and acceptable for the mission, but it is not negligible. The mission average ratio of uncorrectable errors versus SEU is about 0.4%. The cause of these uncorrectable errors is the SMU sensitivity of the HITACHI 1M SRAM device. The same device was flown in the CRUX/APEX experiment, and SMU were also reported [11-13]. This example shows that the risk of SMU needs to be carefully evaluated during ground testing.

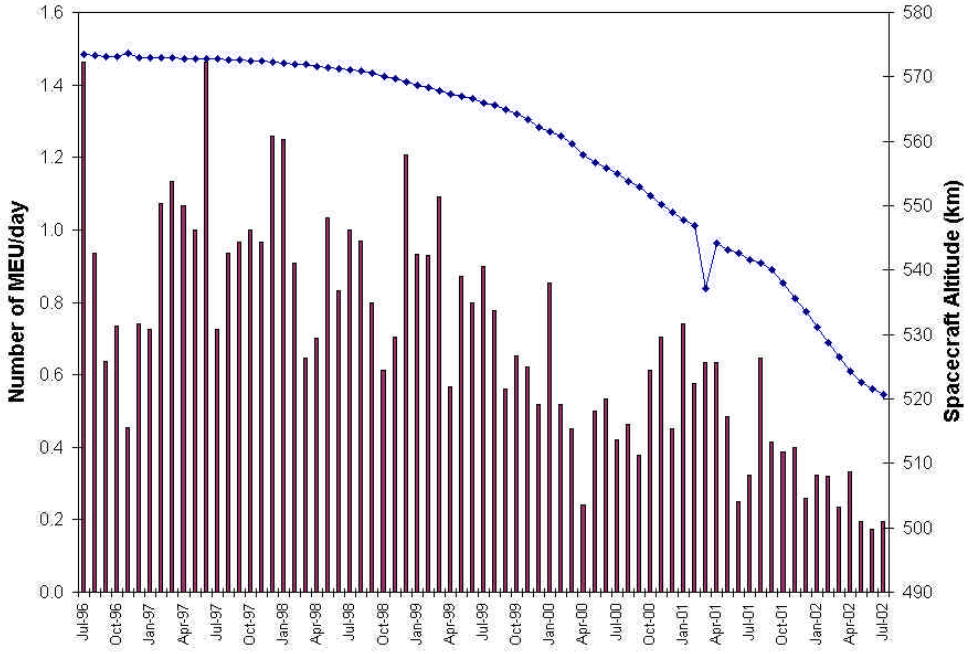

Fig 14: daily number (monthly average) of uncorrectable errors of the XTE SSR.

All Surrey Space Center (SSC) OBCs that used the Hamming (12, 8) code scheme to protect their program storage memories did not have any SEU related problem [3-6]. As the SMU sensitivity has increased in state of the art memory devices, they decided to use a triple modular redundancy (TMR) hardware EDAC scheme to protect the OBC program memory of their most recent micro-satellites FaSat-Bravo, Thai-Phutt, and UOSAT12 [6]. With TMR, any number of bits may be flipped within a byte, the majority voting circuit will out-vote such bit errors, two to one against. This SEU mitigation scheme is very robust, but requires a 200% storage overhead and is therefore limited to small program storage memories. For future systems SSC will use a variant of the Hamming code, a (16, 8) code capable of detecting and correcting up to two bit errors per word. Based on their experience, they consider that this code will cope with the vast majority of SEU with a minimum memory overhead. The APEX/CRUX data on the Hitachi 1M SRAM that all SMU were double bit errors [13]. The implementation of such variant of Hamming code would have suppressed all the uncorrectable errors.

Reed Solomon (RS) EDAC codes are very powerful. NASA has developed a hardware RS (255,223) encoder that is able to correct up to 16 consecutive bytes in error [57]. The particular version used for the HST SSR is a RS (255, 224) is able to correct up to 10 bytes in error in the 224 bytes data structure. The large multiple bit errors observed on HST were fully correctable with this RS EDAC [54]. The old SSC spacecraft [3-6] used a less powerful version RS(255,252) but with less coding overhead for their SSRs. This version is capable of correcting 1 byte in error, and to detect 2 bytes in errors. These double byte uncorrectable errors are reported as severe errors in their data. Data shows a significant number of uncorrectable errors ranging from 1E-10 to 6E-10 per byte day [3-5]. In all cases the ratio of severe errors to correctable errors is less than 1%. In their last generation of micro satellites, Thai-Phutt and UOSAT12, SSC has implemented a RS(256,252) capable of double byte correction. Three or more bytes would have to be affected to cause a severe error under this scheme. With this new scheme the number of uncorrectable errors on UOSAT12 has been reduced from 2E-9 per bit day to 1E-10 per bit day. This represents a twenty fold improvement [6].

4 Lessons learned

4.1 SEU rate

The main lesson learned is that there is large SEU sensitivity range from device to device type, and part to part for the same device type. There is also a large variation of sensitivity depending on the environment. When the flown device has been characterized both to heavy ion and protons, the calculated SEU rate is generally in good agreement with the observed average flight rate (within an order of magnitude) for the background environment. However, the standard assumption of a thin sensitive volume thickness of 2 µm is too conservative for some devices, especially DRAMs. It should also be noted that, despite all the conservative assumptions made for the predictions, these predictions are not always pessimistic. This is generally the result of inaccurate test data, or inaccurate modelization of the radiation environment.
The SPE CREME96 standard models (peak event, worst day, and worst week) give generally very conservative values of the upset rates during a SPE.

4.2 MBU

Flight data shows that the MBU rate is significant (up to 20% of the total event rate). SMU are generally detected during ground testing, but it is generally difficult to quantify accurately the risk because of the large anisotropy of the mechanisms involved [19, 39]

4.3 SEFI

SEFI events have been observed on flight on memories. Because of the low (but not negligible) sensitivity, these types of events can be incorrectly characterized during ground testing of a small number of parts.

4.4 SHE

SHEs due to microdose deposition have been observed in flight. SHE can be detected during ground testing, but again it is very difficult to accurately quantify the risk.
No SHE due to SEGR has been identified. This risk can be detected during ground testing.

4.5 SEL

Only a few part types are sensitive to SEL, but one part has shown an extremely high heavy ion and proton induced SEL sensitivity [26]. This risk can be detected during ground testing.

4.6 SEE mitigation schemes

The coding techniques have shown their efficiency to mitigate SEUs as long as the use of the parts has been carefully considered and the risk of SMU evaluated during ground testing.
Scrubbing rates are generally calculated on the basis of daily average SEU rates. This is adequate for GEO or interplanetary orbits in the absence of SPE. For LEO the data shows that the SEUs occur in burst when the spacecraft goes through the trapped proton belts. For example, on a LEO polar orbit, 80% of the SEU occur in the SAA in bursts lasting for 5 to 10 minutes per orbit. The scrubbing rate needs to be calculated for these high SEU rates.
Only a few SEL and SEFI occurrences have been observed in flight. The memories have recovered full functionality after a power cycling and reinitialisation.
SHEs due to microdose effects disappeared by themselves after a period ranging from seconds to months. As long as the SHE rate (microdose and or SEGR) is low, they can be corrected by the SEU correction codes.

5 Recommendations

5.1 Ground testing

An accurate heavy ion and proton SEE characterization is essential to assess the in flight SEE risk. The best accuracy is obtained when testing is done on parts coming from the flight lot. The sample size is also an important factor. Generally, because of the cost of particle accelerators, the SEE tests are performed on 2 to 3 parts. This gives poor test fidelity. Assuming that SEE sensitivity on memory device follows a binomial law, it is necessary to test 23 parts to get a sensitivity which will not be exceeded with a probability of 90% and a confidence level of 90%. It is important to test the parts not only for SEU, but for all the other potential sensitivities: SMU, SHE, SEFI, and SEL. Generally the statistics, and therefore the accuracy of these tests is poor.
An accurate TID characterization is also important, when the sensitivity is evaluated, the mission dose levels on memories should be kept to a level where no significant degradation is observed. It is essentially important for SSRs applications where a small increase of power supply current on a large number of devices may lead to a significant increase of the SSR supply current.

5.2 SEE error rate calculation

With an accurate heavy and proton characterization, use of the adequate environment models, reasonable assumptions on the sensitive volume thickness, the flight SEU rates will be estimated within an order of magnitude for the background radiation environment.
As shown by the flight data, an orbit average rate does not correspond to the reality where the majority of SEUs occur in bursts (very high rate during a short period of time). These maximum rates need to be calculated.
The SPE environment models will give conservative estimates of the SEU rates during solar events.

For the other events such as SEL, SEFI, SEGR,.., the accuracy of the prediction will be very poor. SEL and SEFI rate calculation assuming only one sensitive volume of area the device SEL cross section and a thickness of 2 um will give a conservative estimate of the flight rates. For SMU rates calculations these assumptions will lead to unrealistically high estimations of the SMU rates and considering every memory cell as a sensitive volume will underestimate the SMU rate. For these events we recommend to apply a higher design margin than for SEU.

5.3 SEE mitigation scheme

5.3.1 SEU and MBU

EDAC techniques work well to mitigate SEU. Hamming code will fail in case of SMU. The obvious and well-known solution to deal with SMU on single bit correction codes is to simply rearrange the memory so that it is constructed from devices with a “x1 bit” architecture. With such an architecture multiple bit flips within a device will be spread across several data words, thus causing no difficulty with the Hamming code EDAC system. Unfortunately recent memories are not available with x1 bit architecture, therefore using only one bit per memory device to form a data word will require a large memory overhead or a complex design. Another solution is the use of a modified Hamming code capable of correcting 2 bits in a data word.
For LEO orbits the data shows that the SEU occur in bursts when the spacecraft goes through the trapped proton belts. For example, on a LEO polar orbit, 80% of the SEU occur in the SAA in bursts lasting for 5 to 10 minutes per orbit. The scrubbing rate needs to be calculated for this high SEU rate. On the other hand, in the absence of SPE, the number of SEUs that occur outside the SAA are so small that they can be ignored. If the scrubbing rate is longer than the time taken to pass through the trapped proton belt, it would be just as effective to make the scrubbing rate equal to the orbital period. If the scrubbing rate is substantially shorter than the time taken to pass through the trapped proton belt, the scrubbing may be suspended for the rest of

the orbit where the spacecraft is outside the trapped proton belt. However, in case of large SPE the SEU rate may also be very high outside the SAA.

5.3.2 Other single events

Use of devices not sensitive to SEL, SEFI, SEGR and SHE is recommended. In SSR applications, because of the large number of devices used, there is always the risk of such an event. It is recommended to use a flexible design, with current limitations, and the possibility to power cycle and reinitialize. The use of spare memory is also useful in case of permanent failure of some parts of the memory array due to SEGR or destructive SEL.

6 Conclusions

COTS memories have been flown with success the last ten years. Memory experiments have been very useful to check the behavior of these parts in space. It is very important because the MBU sensitivity is difficult to test accurately at ground.

State-of-the-art memories, like SDRAMs, are becoming more and more complex, and therefore more difficult to test and more sensitive to radiation effects. New flight experiments on these devices are essential to "secure" the use of these devices in future applications. The flight data has shown that is important to have accurate information about the shielding, and the solar particle flux to study the effects of SPE. As no information is available for solar heavy ions, it is useful to fly a detector with the experiments.

7 References

[1] K. A. LaBel & al., "Solid State Recorders: Spaceflight SEU Data for SAMPEX and TOMS/ Meteor-3," 1993 IEEE Radiation Effects Data Workshop proceedings, pp 1964-1971, 1994.

[2] C.M. Seidleck & al., "Single Event Effect Flight Data Analysis of Multiple NASA Spacecraft and Experiments; Implications to Spacecraft Electrical Designs," RADECS 1995 Proceedings, pp. 581-588, 1996.

[3] C.I. Underwood & al., "Observations of Single Event Upset and Multiple Bit Upset in Non Hardened High-Density SRAMs in the TOPEX/Poseidon Orbit," 1993 IEEE Radiation Effects Data Workshop proceedings, pp 85-92, 1994.

[4] C.I. Underwood , "The Single-Event-Effect Behavior of Commercial-Off-The-Shelf Memory Devices-A Decade in Low-Earth Orbit," ," RADECS 1997 Proceedings, pp. 251-258, 1998.

[5] C.I. Underwood & al., "Observed Radiation-Induced Degradation of Commercial-Off-The Shelf (COTS) Devices Operating in Low-Earth Orbit," IEEE Trans. Nuc. Sci., vol 45, n°6, pp. 2737-2744, Dec. 98.

[6] C.I. Underwood & al., "Observations on the Reliability of COTS-Device-Based Solid State Data Recorders Operating in Low Earth Orbit," RADECS 1999 Proceedings, pp. 387-393, 2000.

[7] E.G. Mullen & al., "SEU Results from the Advanced Photovoltaic and Electronics Experiments (APEX) Satellite," IEEE Trans. Nuc. Sci., vol 42, n°6, pp. 1988-1994, Dec. 95.

[8] R. Harboe-Sorensen & al., "Observation and Analysis of Single Event Effects On-board the SOHO Satellite," RADECS 2001 proceedings, 2001.

[9] T. Goka & al., "SEE Flight Data from Japanese Satellites," IEEE Trans. Nuc. Sci., vol 45, n°6, pp. 2771-2778, Dec. 98.

[10] R. Ecoffet & al., "Influence of Solar Cycle on SPOT1-2-3 Upset Rates," IEEE Trans. Nuc. Sci., vol 42, n°6, pp. 1983-1987, Dec. 95.

[11] J.L. Barth & al., "Single Event Upset Rates on 1 Mbit and 256 Kbit Memories: CRUX Experiment on APEX," IEEE Trans. Nuc. Sci., vol 42, n°6, pp. 1964-1974, Dec. 95.

[12] J. Adolphsen & al., "SEE Data from the APEX Cosmic Ray Upset Experiment: Predicting the Performance of Commercial Devices in Space," RADECS 1995 Proceedings, pp. 572-580, 1996.

[13] J.L. Barth & al., “Single Event Effects on Commercial SRAMs and Power MOSFETs: Final Results of the CRUX Flight Experiment on APEX,” 1998 IEEE Radiation Effects Data Workshop proceedings, pp 1-10, 1998.
[14] D. Falguere & al., “SEE In-Flight Measurement on the MIR Orbital Station,” IEEE Trans. Nuc. Sci., vol 41, n°6, pp. 2346-2352, Dec. 94.
[15] S. Duzellier & al., “EXEQ II et III: Experiences embarquees pour l’etude des evenement singuliers,” RADECS 1997 Proceedings, pp. 504-509, 1998.
[16] D. Falguere & al., “EXEQ I-IV: SEE In-Flight Measurement on the MIR Orbital Station,” 2000 IEEE Radiation Effects Data Workshop proceedings, pp 89-95, 2000.
[17] Ph. Cheynet & al., “Comparison Between Ground Tests and Flight data for two Static 32KB Memories,” RADECS 1999 Proceedings, pp. 554-557, 2000.
[18] S. Duzellier & al., “SEE In-Flight Data for two Static 32KB Memories on High Earth Orbit,” Presented at IEEE NSREC 2002 dataworkshop.
[19] S. Buchner & al., “Investigation of Single-Ion Multiple-Bit Upsets in Memories on Board a Space Experiment,” RADECS 1999 Proceedings, pp. 558-564, 2000.
[20] A. Campbell & al., “SEU Measurement and Predictions on MPTB for a Large Energetic Solar Particle Event,” RADECS 2001 Proceedings.
[21] J. Barak, “Single Event Upsets in the Dual-Port-Board SRAMs of the MPTB Experiment,” RADECS 1999 Proceedings, pp. 582-587, 2000.
[22] D. Falguere & al., “In-Flight Observations of the Radiative Environment and its Effects on Devices in the SAC-C Polar Orbit,” Presented at IEEE NSREC 2002.
[23] D.K. Nichols & al., “Discovery of heavy ion induced Latchup in CMOS/EPI devices,” IEEE Trans. Nuc. Sci., vol 33, n°6, p. 1696, Dec. 86.
[24] T. Chapuis & al., “Latch-up on CMOS/EPI devices,” IEEE Trans. Nuc. Sci., vol 37, n°6, pp. 1839-1842, Dec. 90.
[25] C. Poivey & al., “Radiation Characterization of Commercially available 1Mbit/4Mbit SRAMs for Space Applications,” 1998 IEEE Radiation Effects Data Workshop proceedings, pp 68-73, 1998.
[26] L. Adams & al., “A verified proton induced latchup in space,” IEEE Trans. Nuc. Sci., vol 39, n°6, pp. 1804-1808, Dec. 92.
[27] D.K. Nichols & al., “An observation of proton induced latchup,” IEEE Trans. Nuc. Sci., vol 39, n°6, pp. 1654-1656, Dec. 92.
[28] B. Johlander & al., “Ground verification of in-orbit anomalies in the double probe electric filed experiment on Freja,” IEEE Trans. Nuc. Sci., vol 43, n°6, pp. 2767-2771, Dec. 96.
[29] A. Johnston & al., “Latchup in integrated circuits from energetic protons,” IEEE Trans. Nuc. Sci., vol 44, n°6, pp. 2367-2377, Dec. 97.
[30] R. Koga & al., “On the suitability of non-hardened high density SRAMs for space applications,” IEEE Trans. Nuc. Sci., vol 38, n°6, pp. 1507-1511, Dec. 91.
[31] C. Dufour & al., “Heavy ion induced single hard errors on submicronic memories,” IEEE Trans. Nuc. Sci., vol 39, n°6, pp. 1693-1697, Dec. 92.
[32] T.R. Oldham & al., “Total dose failures in advanced electronics from single ions,” IEEE Trans. Nuc. Sci., vol 40, n°6, pp. 1820-1830, Dec. 93.
[33] G.M. Swift & al., “A new class of single event hard errors,” IEEE Trans. Nuc. Sci., vol 39, n°6, pp. 1804-1808, Dec. 92.
[34] K. LaBel & al., “SEU tests of a 80386 based flight computer/data handling system and of discrete PROM and EEPROM devices, and SEL tests of discrete 80386, 80387, PROM, EEPROM and ASICs,” 1992 IEEE Radiation Effects Data Workshop proceedings, pp 1-11, 1992.
[35] C. Poivey & al., “SEP characterization of 1M EEPROMs from SEEQ and Hybrid Memory,” 1994 IEEE Radiation Effects Data Workshop proceedings, pp 20-25, 1994.
[36] R. Harboe Sorensen, R. Muller, “Radiation testing of UV EPROMs, flash EPROMs and EEPROMs for space applications,” ESA report ESA-QCA0076TS, 1996.
[37] P. Dressendorfer, “An overview of advanced non volatile memory technologies,” 1991 IEEE NSREC short course, 1991.
[38] J.A. Zoutendyk & al., “Characterization of Multiple Bit errors from single ion tracks in integrated circuits,” IEEE Trans. Nuc. Sci., vol 36, n°6, pp. 2267-2274, Dec. 89.

[39] A. Makihara & al., “Analysis of single ion multiple bit upset in high density DRAMs,” IEEE Trans. Nuc. Sci., vol 47, n°6, pp. 2400-2404, Dec. 00.
[40] O. Musseau & al, “Analysis of multiple bit upsets (MBU) in a CMOS SRAM,” IEEE Trans. Nuc. Sci., vol 43, n°6, pp. 2879-2888, Dec. 96.
[41] P. Calvel & al, “Space radiation evaluation of 16 Mbit DRAMs for mass memory applications,” ` IEEE Trans. Nuc. Sci., vol 41, n°6, pp. 2267-2271, Dec. 94.
[42] K. LaBel & al., “Radiation Effect Characterization and Test methods of single chip and multi chip stacked 16 Mbit DRAMs,” IEEE Trans. Nuc. Sci., vol 43, n°6, pp. 2974-2981, Dec. 96.
[43] C. Poivey & al., “Heavy Ion Induced Gicantic Multiple Errors in State of the Art Memories,” 4th ESA Electronic Component Conference (EECC) April 2000, Noordwijk, The Netherlands.
[44] R. Koga & al., “Permanent Single Event Functional Interrupts (SEFIs) in 128 and 256 Megabit Synchronous Dynamic Random Access Memories (SDRAMs),” 2001 IEEE Radiation Effects Data Workshop proceedings, pp 6-13, 2001.
[45] B. Doucin, “AM29(LV/F)800B-120, 8Mbit flash EPROM from AMD, heavy ion and proton SEE test report,” report ref. DOF/DEC/GER/RP7.223, Aug. 97.
[46] C.I Lee & al., “Total ionizing dose effects on 64 Mbit 3.3V DRAMs,” 1997 IEEE Radiation Effects Data Workshop proceedings, pp 97-100, 1997.
[47] C. Poivey & al., “Radiation characterization of commercially available 1Mbit/4Mbit SRAMs for space applications,” 1998 IEEE Radiation Effects Data Workshop proceedings, pp 68-73, 1998.
[48] R. Harboe Sorensen & al., “Radiation evaluation of 3.3V 16Mbit DRAMs for Solid State Memory Space Applications,” 1998 IEEE Radiation Effects Data Workshop proceedings, pp 74-79, 1998.
[49] M.V. O’Bryan & al., “Radiation damage and Single Event Effect Results for Candidate Spacecraft Electronics,” 2000 IEEE Radiation Effects Data Workshop proceedings, pp 106-122, 1994.
[50] “28C256 TID test report” NASA report ppm95-175, 1995.
[51] “28C256 TID test report” NASA report ppm95-169, 1995.
[52] G.M. Swift & al., “In Flight Observations of Multiple Bit Upset in DRAMs,” IEEE Trans. Nuc. Sci., vol 47, n°6, pp. 2386-2391, Dec. 00.
[53] C. Poivey, “Flight data analysis report,”
[54] K.A. LaBel, “Investigation of an in flight anomaly: Investigation of Proton SEE Test Results for Stacked IBM DRAMs,” ,” IEEE Trans. Nuc. Sci., vol 45, n°6, pp. 2898-2903, Dec. 98.
[55] J. Barth, “Modeling Space Radiation Environment,” IEEE NSREC1997 short course, 1997.
[56] C. Dyer & al., “Radiation Environment of the MPTB as measured by CREDO-3,” IEEE Trans. Nuc. Sci., vol 47, n°6, pp. 2208-2217, Dec. 00.
[57] K. LaBel & al., “Single Event Effect Mitigation from a System Perspective,” IEEE Trans. Nuc. Sci., vol 43, n°2, pp. 654-660, Apr. 96.